

Cite this: *Catal. Sci. Technol.*, 2020,  
10, 327Received 22nd September 2019,  
Accepted 17th November 2019

DOI: 10.1039/c9cy01877h

rsc.li/catalysis

## Efficient selective hydrogenation of 2-butyne-1,4-diol to 2-butene-1,4-diol by silicon carbide supported platinum catalyst†

Miao Shu,<sup>ac</sup> Chuang Shi,<sup>d</sup> Jing Yu,<sup>e</sup> Xiao Chen,<sup>id</sup>\*<sup>d</sup>  
Changhai Liang,<sup>id</sup><sup>d</sup> and Rui Si,<sup>id</sup>\*<sup>ab</sup>

Selective hydrogenation of 2-butyne-1,4-diol (BYD) to 2-butene-1,4-diol (BED) is important for chemical industries. In this work, a low concentration (0.5 wt%) of platinum (Pt) was deposited onto a silicon carbide (SiC) support by an incipient wetness impregnation approach, and the as-obtained catalyst exhibited an excellent selectivity (~96%) for BED with a high conversion of 96% for BYD. Multiple characterization techniques were applied to investigate the active species for this reaction. The X-ray absorption fine structure (XAFS) data together with the high-resolution transmission electron microscopy (HRTEM) images indicated that the as-calcined 0.5Pt/SiC consisted of platinum oxide clusters (Pt<sub>x</sub>O<sub>y</sub>), which were further converted to the reduced Pt<sup>0</sup> species during the hydrogenation process. Therefore, metallic Pt nanoparticles with 2–3 nm in size supported on silicon carbide are the active species for BED products *via* the selective hydrogenation of BYD in this work.

2-Butene-1,4-diol (BED) is a type of versatile and important industrial material, and it can be manufactured as the intermediate of medicine, battery, papermaking, leathers, agricultural chemicals, vitamins A and B6.<sup>1,2</sup> Currently, the broadest commercial production method of BED is the selective hydrogenation of 2-butyne-1,4-diol (BYD) by nickel<sup>3–6</sup> or palladium catalysts.<sup>7–15</sup> However, the industrial nickel-based catalysis inclines to undergo full hydrogenation of BYD to butane-1,4-diol (BDO), and normally requires a harsh

condition (15–30 MPa at up to 160 °C).<sup>16–19</sup> Palladium-based catalysts have been studied relatively more, but higher selectivity (>60%) usually requires an adequate high concentration of the noble metal (Pd)<sup>9</sup> or additives.<sup>15</sup>

Recently, platinum-based catalysts also have been investigated for the selective hydrogenation of BYD under mild conditions (<150 °C & <3 MPa) and the related samples showed low selectivity (*ca.* 80%).<sup>20–23</sup> Furthermore, previous results reported that multiple side products, including  $\gamma$ -hydroxy butyraldehyde, *n*-butyraldehyde, *n*-butanol, crotyl alcohol, acetal, 2-isopropoxy-tetrahydrofuran and butane,<sup>12,24</sup> would be generated during the hydrogenation of BYD to BED in practical production.<sup>25</sup> So, suitable modification of support<sup>20,26</sup> or appropriate doping of secondary metal<sup>27,28</sup> becomes an essential challenge for balancing between high activity (especially high selectivity) and low cost (low concentration of noble metal) for the production of BED over the Pt-based catalysts. Particularly, the influence of different supports, including carbonate,<sup>27</sup> carbon,<sup>28</sup> zeolites,<sup>20</sup> and bovine-bone powder<sup>21</sup> has been thoroughly investigated previously. Li *et al.* studied the effect of different molecular sieves and reported the higher selectivity of Pt@ZIF-8 (>90%) compared with the Pt nano-sol and Pt@SBA-15 (<70%).<sup>20</sup> Bennett *et al.* found that the chemically processed biogenic Pt catalyst has a higher selectivity than carbon-supported Pt materials.<sup>28</sup> As a non-oxide support, silicon carbide (SiC) has been used in heterogeneous catalysis, due to its excellent thermal stability, high thermal conductivity and inertness in harsh environments.<sup>29–31</sup> However, until now, SiC-supported Pt catalysts have not been reported for the selective hydrogenation reaction of BYD.

Herein, we have deposited the monometallic platinum with varied loading amounts (0.1, 0.5, 1, 5 wt%) on the silicon carbide support as well as on other supports (silica SiO<sub>2</sub>, silicon nitride SiN, active carbon AC, cerium oxide CeO<sub>2</sub>) by an incipient wetness impregnation method. The catalytic performance of as-obtained samples was evaluated by the selective hydrogenation reaction of BYD to BED. With

<sup>a</sup> Shanghai Institute of Applied Physics, Chinese Academy of Sciences, Shanghai 201800, China. E-mail: sirui@sinap.ac.cn

<sup>b</sup> Shanghai Synchrotron Radiation Facility, Zhangjiang Laboratory, Shanghai 201204, China

<sup>c</sup> University of Chinese Academy of Science, Beijing 10049, China

<sup>d</sup> State Key Laboratory of Fine Chemical & Laboratory of Advanced Materials and Catalytic Engineering, School of Chemical Engineering, Dalian University of Technology, Dalian 116012, China. E-mail: xiaochen@dlut.edu.cn

<sup>e</sup> Shanghai Institute of Measurement and Testing Technology, Shanghai 200233, China

† Electronic supplementary information (ESI) available. See DOI: 10.1039/c9cy01877h

the help of multiple structural characterizations, including high-resolution transmission electron microscopy (HRTEM) and X-ray absorption fine structure (XAFS) spectra, we have further investigated the active species for the reactivity of selective hydrogenation of BYD to BED.

The selective hydrogenation of BYD was used to evaluate the catalytic performance of the supported platinum catalysts. Mild reaction conditions (100 °C,  $p(\text{H}_2) = 1 \text{ MPa}$ , 10 h) were applied in the batch reactor. Fig. 1a shows the comparison of conversion and selectivity for all the measured catalysts. First, the effect of the loading amount of Pt was investigated. Fig. 1a determines that the highest selectivity of BED appeared for 0.1Pt/SiC (98%), followed by 0.5Pt/SiC (96%), 1Pt/SiC (94%) and 5Pt/SiC (92%), respectively (also refer to Fig. S1a†). However, the trend of conversion was totally different. Fig. 1a (also refer to Fig. S1b†) exhibits that the conversion of BYD for 0.5Pt/SiC (*ca.* 96%) was higher than that of the 1Pt/SiC (94%), 0.1Pt/SiC (87%) and 5Pt/SiC (81%). Therefore, 0.5Pt/SiC can be selected as the primary catalyst for further investigations due to its simultaneous high conversion and high selectivity.

The effect of the loading amount of Pt on the conversion of BYD and selectivity of BED also were investigated as the function of reaction time (Fig. S2a†). The 5Pt/SiC almost has the same conversion (*ca.* 24%) in the initial 2 h reaction, which was slightly higher than that of 0.5Pt/SiC (20% conversion). With the reaction progressing, the conversion of BYD for 0.5Pt/SiC caught up to 96% after 10 h, approximate to that of 1Pt/SiC and significantly higher than that of 0.1Pt/SiC and 5Pt/SiC. Fig. S2b† exhibits that all the four samples with different loadings of Pt almost remained unchanged for selectivity of BED within the 10 h reaction.

We further compared the activity of Pt-based catalysts in different kinds of literature on the selective hydrogenation of BYD. Table 1 shows that 0.5Pt/SiC synthesized in this work attained the similar selectivity of BED as Pt@ZIF-8 (96%)<sup>20</sup> but under lower  $\text{H}_2$  pressure and loading of Pt. Although 0.5Pt/SiC progressed at a higher temperature than the reported  $\text{CaCO}_3$  supported Pt catalysts with  $\text{NH}_3$  pretreatment<sup>26</sup> or Li addition,<sup>27</sup> the current concentration of platinum was only half and without any extra operation for catalysts. To better explore the effect of the supports, we deposited 0.5 wt% Pt on different supports such as silica

( $\text{SiO}_2$ ), silicon nitride (SiN), active carbon (AC), and cerium oxide ( $\text{CeO}_2$ ) by the same incipient wetness impregnation approach. Fig. 1a shows that 0.5Pt/SiN has the best conversion of BYD (almost 100%), while the related selectivity of BED was the lowest (~78%) in all the measured catalysts. Importantly, platinum supported on other support has the lower selectivity of BED (<91%) than the Pt/SiC series (92–98%). Therefore, these results give sufficient evidence that silicon carbide was the best support for the platinum catalysts to the selective hydrogenation reaction of BYD to BED in our research. Remarkably, the reaction products consisted of only one side-compound (BDO), which is an advantage, if compared to the previously reported Pt-based catalysts with a high selectivity of BED above 96%.<sup>20,21</sup>

The recyclability of 0.5Pt/SiC was operated at 100 °C and  $p(\text{H}_2) = 1 \text{ MPa}$  to verify the stability of investigated platinum catalysts. Fig. 1b displays that 0.5Pt/SiC holds good reproducible catalytic performance with a high conversion of BYD (99%, 99%, and 95%) and good selectivity of BED (85%, 82%, and 86%) for the three runs. These data were collected offline and the slight decrease in the selectivity should be related to the separation and transformation of catalyst powders from the stock solution, compared to the online sample collections (Fig. 1a).

Besides, the effect of the pretreatment condition was also investigated. Fig. S3† confirms that the  $\text{O}_2$ -pretreated catalyst showed a nearly identical conversion of BYD and selectivity of BED compared to the  $\text{H}_2$ -pretreated 0.5Pt/SiC. This is because flushing with  $\text{H}_2$  in a batch reactor to eliminate the dissolved air as well as the initial reaction period at 100 °C with 1 MPa  $\text{H}_2$  effectively reduced the  $\text{O}_2$ -pretreated catalyst. Thus, during the reaction, there was only one status for platinum ( $\text{Pt}^0$ ), whether  $\text{H}_2$ - or  $\text{O}_2$ -pretreatment. As discussed above, the comparison of activity over the various Pt-based catalysts for the hydrogenation of BYD to BED in this work has been summarized in Table S1†.

Multiple characterization techniques were used to discover the origin of catalytic reactivity over silicon carbide supported platinum catalysts. Table S2† shows that the experimental concentration of Pt was 0.39 wt% for both fresh and used 0.5Pt/SiC, which is in good agreement with the designed value (0.5 wt%). The  $\text{N}_2$  adsorption/desorption measurement was used to identify the textural properties of these samples under different status (as-purchased SiC, SiC with deionized water, fresh and used 0.5Pt/SiC). Fig. S4a† exhibits a type IV isotherm and the H3 type hysteresis loop, attributed to the presence of aggregated particles.<sup>32</sup> Table S2† shows that the BET specific surface areas ( $S_{\text{BET}}$ ) were almost constant (*ca.* 30  $\text{m}^2 \text{ g}^{-1}$ ). On the contrary, the BJH pore volumes ( $V_{\text{p}}$ ), which appeared like that of the as-purchased SiC was only 0.071  $\text{cm}^3 \text{ g}^{-1}$ , significantly less than that for immersed SiC (0.162  $\text{cm}^3 \text{ g}^{-1}$ ) or fresh/used 0.5Pt/SiC. The BJH average diameters in Fig. S4b† display a similar trend, *i.e.* the diameter of the as-purchased SiC (17 nm) was lower than that of the immersed one (SiC-IMP, 36 nm) or fresh/used 0.5Pt/SiC. These results indicate that the transformation of textural

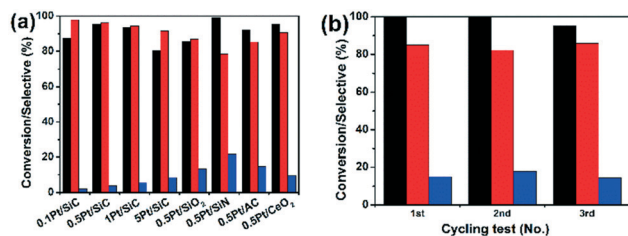


Fig. 1 (a) Comparison on conversion and selectivity for catalysts with different Pt loadings or different supports; (b) recyclability for 0.5Pt/SiC at 100 °C and  $p(\text{H}_2) = 1 \text{ MPa}$  (black: conversion of BYD; red: selectivity of BED; blue: selectivity of BDO).

**Table 1** Comparison on the activity over the Pt-based catalysts in literatures for selective hydrogenation of 2-butyne-1,4-diol reaction (BYD) to 2-butene-1,4-diol (BED) (solvent: H<sub>2</sub>O)

Catalyst	Pt loading (wt%)	Reaction condition	BYD conversion (%)	BED selectivity (%)	Ref.
Pt/SiC	0.5	100 °C; 1 MPa	96	96	This work
Pt@ZIF-8	1	120 °C; 3 MPa	100	94	20
Pt nano-sol	1	120 °C; 3 MPa	~95	68	20
Pt@SBA-15	1	120 °C; 3 MPa	~100	68	20
Pt/bovine-bone	1	55 °C; 0.6 MPa	~100	83	21
Pt/CaCO <sub>3</sub>	1	50 °C; 2.4 MPa	~95	83	26
Pt/CaCO <sub>3</sub> -NH <sub>3</sub>	1	50 °C; 2.4 MPa	—	100	26
Pt-Li/CaCO <sub>3</sub>	1	50 °C; 2.4 MPa	99.6	83	27
Pt-Cs/CaCO <sub>3</sub>	1	50 °C; 2.4 MPa	—	99	27
Pt/PANI	2	22 °C; 0.1 MPa	85	75	22
Pt/P4VP	4	22 °C; 0.1 MPa	85	80	23

properties for the SiC support was derived from the impregnation step with the water solvent.

To better understand the structural evolution by the deposition of Pt over SiC, we performed the related structural characterization techniques. The powder X-ray diffraction (XRD) patterns in Fig. 2 determined the main peaks at 35.6°, 41.4°, 60.0°, 71.8°, and 75.6°, which corresponded to the (111), (200), (220), (311), and (222) facets of cubic  $\beta$ -SiC (JCPDS card no.: 29-1129), respectively. The appearance of two additional peaks at 33.7° and 38.2° can be attributed to the stacking faults (SF) inside the  $\beta$ -SiC materials.<sup>33–35</sup> Apparently, the peak at 39.8° enlarged in Fig. 2b emerges when the loading amount of Pt increases to 0.5 wt%, which can be assigned to the Pt (111) facet (JCPDS card no.: 4-802). This Pt diffraction peak was enhanced with the loading amount of Pt, giving a hint that the Pt crystal size on SiC was generally increased with the loading amount of Pt.<sup>36</sup> Meanwhile, the Fig. 1a shows the selectivity of BED was decreased with the the increased loading of Pt, which suggests that the larger size of Pt specials has a negative effect on the selectivity for the selective hydrogenation of BYD reaction.

Furthermore, the used 0.5Pt/SiC after three recycling tests also was characterized by XRD. Fig. 2c showed that there was nearly no significant difference between the fresh and used samples, revealing that the SiC support was structurally stable during the hydrogenation reaction. Besides, Fig. 2d defined that the Pt peak of used 0.5Pt/SiC was stronger than that of the fresh one, indicating the sequential reduction of platinum species during the reaction.

The thermogravimetric analysis (TGA) was applied to study the thermal stability of silicon carbide supported platinum catalysts.<sup>37</sup> Fig. S5† showed in general that for both the fresh and used samples, the weight loss before 150 °C belongs to the removal of surface water adsorbed on the catalyst, while the weight loss after 500 °C responded to the loss of crystal water. Furthermore, the significantly increased weight loss for the used catalysts between 150 and 500 °C can be attributed to the burning of C<sub>4+</sub> substances (BYD, BED, BDO),<sup>38</sup> which originated from the adsorption of substrates during the reaction.

The morphologies of the support as well as the particle sizes of the metal were determined by TEM/HRTEM images that are presented in Fig. 3, which reveal the well-distributed Pt nanoparticles deposited on the SiC thin layer. Based on the HRTEM images, the average Pt sizes of fresh and used

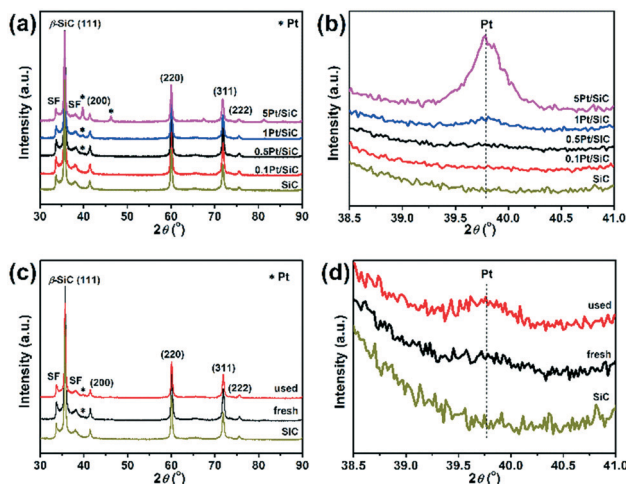


**Fig. 2** XRD patterns in full range (a and c) and enlarged range (b and d) for (a and b) different Pt loadings and (c and d) SiC, as well as 0.5Pt/SiC before and after the reaction.

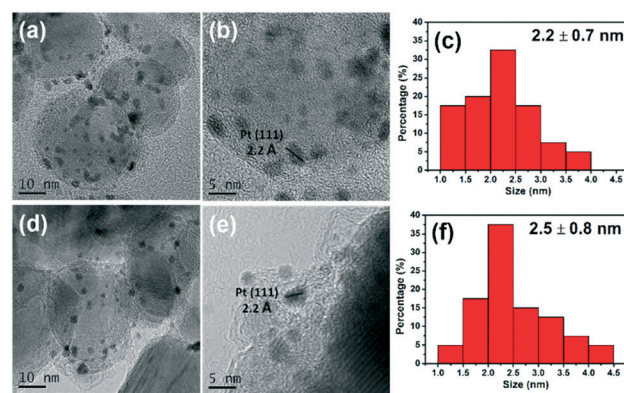


**Fig. 3** TEM (a and d), HRTEM (b and e) images and Pt particle size-distribution histograms (c and f) for 0.5Pt/SiC: (a–c) fresh and (d–f) used after reaction.

catalysts were 2.2 and 2.5 nm, respectively. Meanwhile, Fig. S6† exhibited that the average size of Pt particles was 2.5 nm for 1Pt/SiC. In addition, there were no visible Pt crystals for 0.1Pt/SiC, which matches well with the XRD pattern (Fig. 2b). On the contrary, non-uniform Pt particles (larger than 20 nm, as well as a few in nanometer-scale) appeared for 5Pt/SiC, corresponding to the further growth of platinum species in a high Pt loading sample (also see XRD pattern in Fig. 2b).<sup>36</sup> These experimental results revealed that the Pt size has a significant effect on the catalytic performance on the selective hydrogenation of BYD. Nevertheless, the effect of Pt size was not connected to the type of support. The TEM and HRTEM images shown in Fig. S7† confirmed that the same loading amount of Pt (0.5 wt%) has a different Pt size if supported on different supports. For 0.5Pt/SiN, the average size of platinum was the same as 0.5Pt/SiC (2.2 nm), but the former showed the lowest selectivity among all the studied supports (Fig. 1a). As for 0.5Pt/AC and 0.5Pt/CeO<sub>2</sub>, there were no obvious Pt particles in TEM/HRTEM, probably in atoms or ultra-thin clusters but their selectivity of BED was also lower than that of 0.5Pt/SiC (Fig. 1a). Therefore, according to the present results from Fig. S6 and S7† and 1a, we could draw a conclusion that the selectivity of BED was determined by both the type of the support and the size of Pt.

Since the conventional characterization techniques failed to provide the information on the electronic structure and local coordination structure around the active metal (Pt), we further applied the XAFS measurements on these silicon carbide support platinum catalysts. Fig. 4a exhibited that the X-ray absorption near edge spectroscopy (XANES) profiles of Pt L<sub>3</sub> edge responded to the platinum oxidation state of tested samples, the high intensity of white peak indicating the high valence state of Pt<sup>2+</sup> or Pt<sup>4+</sup>. The corresponding linear combination fitting<sup>39</sup> results shown in Table S3† confirms that the oxidation states of platinum are +1.7 and +0.1 for the fresh and used catalysts, respectively. In other words, platinum was nearly in the Pt<sup>2+</sup> state for the fresh catalyst, while almost pure Pt<sup>0</sup> was identified after the hydrogenation reaction. According to the results of XRD, HRTEM and XANES, we can infer that the fresh sample consisted of both Pt<sup>0</sup> particles and Pt<sub>x</sub>O<sub>y</sub> species (probably on the surface of platinum metals), while the latter oxidized component was converted to metallic platinum fraction during the reaction. In order to further clarify the structural evolution of silicon carbide supported platinum catalysts, the

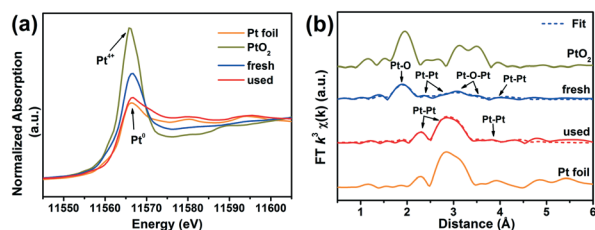


Fig. 4 (a) XANES profiles; (b) Fourier transform of  $k^3$ -weighted EXAFS spectra in  $R$  space of Pt L<sub>III</sub> edge for fresh and used 0.5Pt/SiC.



Scheme 1 Schematic presentation on structural evolution of Pt/SiC catalyst for selective hydrogenation of 2-butyne-1,4-diol reaction (BYD) to 2-butene-1,4-diol (BED).

extended X-ray absorption fine structure (EXAFS) spectra with the related fits were used to identify the local coordination structure containing distance ( $R$ ) and coordination number (CN) around the platinum atoms. Fig. 4b, as well as Table S3† verifies that the fresh 0.5Pt/SiC contains two contributions from the first-shell of Pt–O (2.01 Å) and second-shell of Pt–Pt from the Pt–O–Pt structure (3.1 Å), which is well consistent with the structural properties of Pt<sub>x</sub>O<sub>y</sub> clusters.<sup>39</sup> In addition, the existence of Pt–Pt metallic bonds at 2.79 and 3.95 Å confirms the presence of Pt<sup>0</sup> particles. For the used 0.5Pt/SiC, only the Pt–Pt shell (2.76 and 3.93 Å) appeared without any component of Pt–O, in good agreement with the transformation of oxidized Pt<sub>x</sub>O<sub>y</sub> clusters to reduced Pt particles under the reaction conditions.

In addition, due to the low loading amount of Pt and only a part of it being reducible Pt<sub>x</sub>O<sub>y</sub> clusters, there was no observable temperature-programmed reduction by the hydrogen (H<sub>2</sub>-TPR) peaks (see Fig. S8†) for fresh 0.5Pt/SiC, which manifests no strong metal (Pt)–support (SiC) interaction in this system. Meanwhile, the EXAFS spectrum as well as the corresponding fit (Fig. 4b) discloses that no Pt–Si shell in the range of 3–4 Å, originated from Pt–O–Si interaction, can be identified. This coincided well with the H<sub>2</sub>-TPR results. Consequently, combining with the evaluation of the hydrogenation of BYD, we deem that the reduced Pt nanoparticles themselves are the active species for the high activity, especially high selectivity for BED.

With the help of multiple characterization techniques, the structural evolution of silicon carbide supported platinum catalysts for the selective hydrogenation of BYD can be described in Scheme 1. The oxidized Pt<sub>x</sub>O<sub>y</sub> species and the reduced Pt<sup>0</sup> species (2–3 nm) are coexisting on SiC for the fresh catalyst, and the former was totally reduced under the H<sub>2</sub>-pretreatment condition. The small-size metallic Pt nanoparticles play the key roles in the efficient selective hydrogenation of BYD to BED with high selectivity under 100 °C and  $p(\text{H}_2) = 1$  MPa.

## Conclusions

In summary, we prepared a series of new silicon carbide supported platinum catalysts *via* a simple approach of incipient wetness impregnation. The as-obtained samples were evaluated by the selective hydrogenation of BYD. Importantly, we found that the selectivity of BED was affected

by both the size of Pt and the type of the support. Specifically, the Pt/SiC catalyst with a low loading amount of Pt (0.5 wt%) exhibited an outstanding selectivity of BED (up to 96%) with excellent conversion (up to 96%) under 100 °C and  $p(\text{H}_2) = 1$  MPa after 10 h reaction. The side product was only BDO, which may be beneficial to the reaction operation and the sequential separation process. With the help of HRTEM and XAFS characterizations, we have clearly demonstrated that the small-size (2–3 nm) metallic Pt particles are the active species for the selective hydrogenation of BYD to BED.

## Conflicts of interest

There are no conflicts of interest to declare.

## Acknowledgements

Financial support from the National Science Foundation of China (NSFC) (21773288, U1932119), National Key Basic Research Program of China (2017YFA0403402) and Fundamental Research Funds for the Central Universities (DUT18GJ206).

## Notes and references

- J. M. Winterbottom, H. Marwan, J. Viladevall, S. Sharma and S. Raymahasay, *Stud. Surf. Sci. Catal.*, 1997, **108**, 59–66.
- R. Natividad, R. Kulkarni, K. Nuithitikul, S. Raymahasay, J. Wood and J. M. Winterbottom, *Chem. Eng. Sci.*, 2004, **59**, 5431–5438.
- J. M. Campelo, R. G. Guardefio, D. Luna, J. M. Marinas, J. Morales and J. L. Tirado, *J. Mol. Catal.*, 1993, **85**, 305–325.
- S. Tanielyan, S. Schmidt, N. Marin, G. Alvez and R. Augustine, *Top. Catal.*, 2010, **53**, 1145–1149.
- H. T. Li, Y. X. Zhao, C. G. Gao, Y. Z. Wang, Z. J. Sun and X. Y. Liang, *Chem. Eng. J.*, 2012, **181**, 501–507.
- X. Chen, M. Zhang, K. Yang, C. T. Williams and C. Liang, *Catal. Lett.*, 2014, **144**, 1118–1126.
- T. Fukuda, *Bull. Chem. Soc. Jpn.*, 1958, **31**, 343–347.
- R. V. Chaudhari, M. G. Parande, P. A. Ramachandran, P. H. Brahme, H. G. Vadgaonkar and R. Jaganathan, *AIChE J.*, 1985, **31**, 1891–1903.
- R. V. Chaudhari, R. Jaganathan, D. S. Kolhe, G. Emig and H. Hofmann, *Appl. Catal.*, 1987, **29**, 141–159.
- M. M. Telkar, C. V. Rode, V. H. Rane, R. Jaganathan and R. V. Chaudhari, *Appl. Catal., A*, 2001, **216**, 13–22.
- M. M. Telkar, C. V. Rode, R. V. Chaudhari, S. S. Joshi and A. M. Nalawade, *Appl. Catal., A*, 2004, **273**, 11–19.
- I. T. Duncanson, I. W. Sutherland, B. Cullen, S. D. Jackson and D. Lennon, *Catal. Lett.*, 2005, **103**, 195–199.
- J. M. Nadgeri, M. M. Telkar and C. V. Rode, *Catal. Commun.*, 2008, **9**, 441–446.
- C. V. Rode, *J. Jpn. Pet. Inst.*, 2008, **51**, 119–133.
- C. Berguerand, I. Yuranov, F. Cardenas-Lizana, T. Yuranova and L. Kiwi-Minsker, *J. Phys. Chem. C*, 2014, **118**, 12250–12259.
- C. J. S. Appleyard and J. F. C. Gartshore, *BIOS Report*, 1946, p. 22.
- S. Rudoff and W. Dethomas, *US Pat.*, US19730346657, 1976.
- R. V. Chaudhari, C. V. Rode, M. M. Telkar, R. Jaganathan and V. H. Rane, *US Pat.*, US6528689B2, 2003.
- N. P. Ward, *CN Pat.*, CN106232561(A), 2016.
- C. Li, M. M. Zhang, X. Di, D. D. Yin, W. Z. Li and C. H. Liang, *Chin. J. Catal.*, 2016, **37**, 1555–1561.
- S. A. Gama-Lara, R. A. Morales-Luckie, L. Argueta-Figueroa, J. P. Hinestroza, I. Garcia-Orozco and R. Natividad, *J. Nanomater.*, 2018, **2018**, 1–8.
- A. Drelinkiewicz, A. Zieba, J. W. Sobczak, M. Bonarowska, Z. Karpinski, A. Waksmundzka-Gora and J. Stejskal, *React. Funct. Polym.*, 2009, **69**, 630–642.
- A. Drelinkiewicz, J. W. Sobczak, E. Sobczak, M. Krawczyk, A. Zięba and A. Waksmundzka-Góra, *Mater. Chem. Phys.*, 2009, **114**, 763–773.
- M. G. Musolino, C. M. S. Cutrupi, A. Donato, D. Pietropaolo and R. Pietropaolo, *J. Mol. Catal. A: Chem.*, 2003, **195**, 147–157.
- G. C. Bond, G. Webb, P. B. Wells and J. M. Winterbottom, *J. Catal.*, 1962, **1**, 74–84.
- M. M. Telkar, C. V. Rode, R. Jaganathan, V. H. Rane and R. V. Chaudhari, *J. Mol. Catal. A: Chem.*, 2002, **187**, 81–93.
- M. M. Telkar, C. V. Rode, V. H. Rane and R. Chaudhari, *Catal. Commun.*, 2005, **6**, 725–730.
- J. A. Bennett, G. A. Attard, K. Deplanche, M. Casadesus, S. E. Huxter, L. E. Macaskie and J. Wood, *ACS Catal.*, 2012, **2**, 504–511.
- M. J. Ledoux, C. Pham-Huu, N. Keller, J. B. Nougayrede, S. Savin-Poncet and J. Bousquet, *Catal. Today*, 2000, **61**, 157–163.
- L. Pesant, J. Matta, F. Garin, M.-J. Ledoux, P. Bernhardt, C. Pham and C. Pham-Huu, *Appl. Catal., A*, 2004, **266**, 21–27.
- L. Fang, X. P. Huang, F. J. Vidal-Iglesias, Y. P. Liu and X. L. Wang, *Electrochem. Commun.*, 2011, **13**, 1309–1312.
- K. S. W. Sing, D. H. Everett, R. A. W. Haul, L. Moscou, R. A. Pierotti, J. Rouquerol and T. Siemieniowska, *Pure Appl. Chem.*, 1985, **57**, 603–619.
- V. V. Pujar and J. D. Cawley, *J. Am. Ceram. Soc.*, 1995, **78**, 774–782.
- V. V. Pujar and J. D. Cawley, *J. Am. Ceram. Soc.*, 1997, **80**, 1653–1662.
- V. V. Pujar and J. D. Cawley, *J. Am. Ceram. Soc.*, 2001, **84**, 2645–2651.
- Y.-X. Tuo, L.-J. Shi, H.-Y. Cheng, Y.-A. Zhu, M.-L. Yang, J. Xu, Y.-F. Han, P. Li and W.-K. Yuan, *J. Catal.*, 2018, **360**, 175–186.
- S. Y. Lee, H. Jung, W. J. Kim, Y. G. Shul and K.-D. Jung, *Int. J. Hydrogen Energy*, 2013, **38**, 6205–6209.
- L. Beneš, K. Melánová and V. Zima, *J. Solid State Chem.*, 2000, **151**, 225–230.
- B. Nan, X.-C. Hu, X. Wang, C.-J. Jia, C. Ma, M.-X. Li and R. Si, *J. Phys. Chem. C*, 2017, **121**, 25805–25817.